

# QKFormer: Hierarchical Spiking Transformer using Q-K Attention

Chenlin Zhou<sup>1\*</sup>, Han Zhang<sup>1,2\*</sup>, Zhaokun Zhou<sup>1,3\*</sup>, Liutao Yu<sup>1</sup>, Liwei Huang<sup>1,3</sup>  
Xiaopeng Fan<sup>1,2</sup>, Li Yuan<sup>1,3</sup>, Zhengyu Ma<sup>1†</sup>, Huihui Zhou<sup>1†</sup>, Yonghong Tian<sup>1,3</sup>

<sup>1</sup>Peng Cheng Laboratory

<sup>2</sup>Harbin Institute of Technology

<sup>3</sup>Peking University

{zhouchl, mazhy, zhouhh}@pcl.ac.cn

## Abstract

Spiking Transformers, which integrate Spiking Neural Networks (SNNs) with Transformer architectures, have attracted significant attention due to their potential for energy efficiency and high performance. However, existing models in this domain still suffer from suboptimal performance. We introduce several innovations to improve the performance: i) We propose a novel spike-form Q-K attention mechanism, tailored for SNNs, which efficiently models the importance of token or channel dimensions through binary vectors with linear complexity. ii) We incorporate the hierarchical structure, which significantly benefits the performance of both the brain and artificial neural networks, into spiking transformers to obtain multi-scale spiking representation. iii) We design a versatile and powerful patch embedding module with a deformed shortcut specifically for spiking transformers. Together, we develop QKFormer, a hierarchical spiking transformer based on Q-K attention with direct training. QKFormer shows significantly superior performance over existing state-of-the-art SNN models on various mainstream datasets. Notably, with comparable size to Spikformer (66.34 M, 74.81%), QKFormer (64.96 M) achieves a groundbreaking top-1 accuracy of **85.65%** on ImageNet-1k, substantially outperforming Spikformer by **10.84%**. To our best knowledge, this is the first time that directly training SNNs have exceeded 85% accuracy on ImageNet-1K. The code and models are publicly available at <https://github.com/zhouchenlin2096/QKFormer>.

## 1 Introduction

Regarded as the third generation of neural networks [Maass, 1997], the brain-inspired Spiking Neural Networks (SNNs) are potential competitors to Artificial Neural Networks (ANNs) due to their high biological plausibility, event-driven properties and low power consumption on neuro-

morphic hardware [Roy *et al.*, 2019]. Spiking Transformers (Transformer-based SNNs) [Zhou *et al.*, 2023c; Zhou *et al.*, 2023a; Yao *et al.*, 2023; Zhou *et al.*, 2023b; Wang *et al.*, 2023], which integrate spiking neural networks with transformer architecture, have attracted significant attention. This innovative combination provides great potential to break through the performance bottleneck of SNNs. However, the performance of existing spiking transformers is still limited for vision tasks on complex datasets, such as on ImageNet.

Spiking Self Attention (SSA) [Zhou *et al.*, 2023c], the core module of spiking transformers, is a novel spike-form self-attention using sparse spike-form Query, key, and Value. However, the computational complexity (especially space complexity) of SSA, scales quadratically to the number of tokens (#tokens). In addition, directly training SNNs needs to unfold the network in the time dimension. Taken together, these two factors indicate huge space consumption burden for training a transformer-based SNN. The multi-scale, hierarchical modular structure, a prominent feature in both the human brain and deep neural networks (DNNs), plays a crucial role in human cognitive functions [Wang *et al.*, 2021] and in vision tasks solved by DNNs. However, existing direct training spiking transformers are all based on the straight-through structure with a fixed small token scale [Zhou *et al.*, 2023c; Yao *et al.*, 2023; Wang *et al.*, 2023], lacking hierarchical spiking representation for downstream vision tasks. The high computational complexity of SSA is the main obstacle to explore hierarchical architecture with fine-grained spiking feature maps in spiking transformers.

To address these issues, we propose a novel hierarchical spiking transformer using Q-K attention for direct training, named QKFormer. Q-K attention, the key module of QKFormer, could efficiently model the importance of token or channel dimensions through binary vectors with linear complexity and only adopts two spike-form components: Query ( $Q$ ) and Key ( $K$ ). QKFormer conducts a hierarchical spiking representation by starting from small patches and gradually merging neighboring patches in deeper spiking transformer layers, with gradually decreasing #tokens. In addition, we design a versatile and powerful patch embedding module with a deformed shortcut specifically for spiking transformers. These merits make QKFormer the most powerful SNN model, in contrast to the previous transformer-based SNNs with spiking feature maps of a single resolution and quadratic

\*Equal contribution.

†Corresponding author.

computational complexity. The main contributions of this paper are as follows:

- We develop a novel spike-form Q-K attention mechanism, tailor-made for the spatio-temporal spiking patterns of SNNs, which can easily model the importance of token or channel dimensions with binary values. The Q-K attention has linear complexity to #tokens (or #channels) and only adopts two spike-form components: Query ( $Q$ ) and Key ( $K$ ).
- We design a versatile and powerful Patch Embedding module with a Deformed Shortcut (PEDS), which enhances spiking information transmission thus improving the performance of spiking transformers greatly.
- We build the hierarchical spiking transformer based on the proposed Q-K attention and PEDS in a direct training way, named QKFormer. This marks the effective exploration of hierarchical spiking representation in Transformer-based SNNs.
- Extensive experiments show that the proposed model outperforms the state-of-the-art (SOTA) SNNs on several static and neuromorphic datasets. Notably, QKFormer has achieved a significant milestone, surpassing **85%** top-1 accuracy on ImageNet with 4 time steps using the direct training approach for the first time.

## 2 Related Work

### 2.1 Convolution-based Spiking Neural Networks.

At present, there are mainly two ways to obtain trained SNNs. One involves converting pre-trained ANNs to SNNs [Bu *et al.*, 2021; Li *et al.*, 2021; Hao *et al.*, 2023], replacing the ReLU activation function in ANN with spiking neurons, resulting in comparable performance to ANNs but with high latency. Another method is to directly train SNNs [Wu *et al.*, 2018], using surrogate gradient [Neftci *et al.*, 2019] [Xiao *et al.*, 2021] to address the non-differentiability of spike excitation function during backpropagation, which results in low latency but relatively poor performance with performance degradation and gradient explosion/vanishing problems. [Zheng *et al.*, 2021] proposed a threshold-dependent batch normalization (tdBN) method, which mitigated the problem of gradient explosion/vanishing, extended directly trained SNNs to 50 layers for the first time, and achieved 67.05 % accuracy with 6 time step on ImageNet. [Fang *et al.*, 2021a] proposed the Spike-Element-Wise block, which further addressed gradient explosion and gradient vanishing problems, and prolonged the directly trained SNNs beyond a depth of 100 layers. MS-ResNet [Hu *et al.*, 2021] directly trained convolution-based SNNs with pre-activation shortcut to successfully extend the depth up to 482 layers on CIFAR10 without experiencing degradation problems.

### 2.2 Transformer-based Spiking Neural Networks.

Transformers [Vaswani *et al.*, 2017] have become benchmark models for natural language processing tasks since it was proposed. Later, Dosovitskiy *et al.* developed Vision Transformer (ViT) [Dosovitskiy *et al.*, 2020], which gradually be-

came a mainstream visual network model with its superior performance.

In terms of transformer-based SNNs, Spikformer [Zhou *et al.*, 2023c] designed a novel spike-form self-attention named Spiking Self Attention (SSA), using sparse spike-form Query, Key, and Value without softmax operation, which was used to construct the Spikformer. Spikformer achieved 74.81% accuracy on ImageNet-1k with 4 time steps, showing the great potential of transformer-based SNNs for the first time. Spikingformer [Zhou *et al.*, 2023a] modified Spikformer with a pre-activation shortcut, which can avoid the floating-point multiplications in synaptic computing and has a lower firing rate. CML [Zhou *et al.*, 2023b] proposed SNN-optimized downsampling to solve the imprecise gradient backpropagation problem in deep SNNs (including Spikformer). CML achieved 77.34% on ImageNet, significantly enhancing the performance of transformer-based SNNs. [Yao *et al.*, 2023] designed a novel Spike-Driven Self-Attention (SDSA), which used only masks and addition operations without any multiplication, thus significantly reducing the computation energy up to an 87.2-fold decrease compared to the vanilla self-attention. [Wang *et al.*, 2023] proposed an SNN-based spatiotemporal self-attention (STSA) mechanism, which calculates the feature dependence across both time and space domains without destroying the asynchronous transmission property of SNNs.

## 3 Method

### 3.1 Preliminary

#### Spiking Neuron Model

Spiking neuron is the fundamental unit of SNNs, we choose Leaky Integrate-and-Fire (LIF) model as the spiking neuron in our work. The dynamics of a LIF neuron can be formulated as follows:

$$H[t] = V[t - 1] + \frac{1}{\tau} (X[t] - (V[t - 1] - V_{\text{reset}})), \quad (1)$$

$$S[t] = \Theta(H[t] - V_{th}), \quad (2)$$

$$V[t] = H[t](1 - S[t]) + V_{\text{reset}} S[t], \quad (3)$$

where  $\tau$  is the membrane time constant, and  $X[t]$  is the input current at time step  $t$ . When the membrane potential  $H[t]$  exceeds the firing threshold  $V_{th}$ , the spiking neuron will trigger a spike  $S[t]$ .  $\Theta(v)$  is the Heaviside step function, which equals to 1 when  $v \geq 0$  and 0 otherwise.  $V[t]$  represents the membrane potential after the triggered event, which equals to  $H[t]$  if no spike is generated and otherwise equals to the reset potential  $V_{\text{reset}}$ .

#### Vanilla Self Attention

Vanilla self-attention (VSA) [Vaswani *et al.*, 2017] in transformers has three floating-point key components: query ( $Q_{\mathcal{F}}$ ), key ( $K_{\mathcal{F}}$ ), value ( $V_{\mathcal{F}}$ ) which are calculated by learnable linear matrices and input  $X$ . The calculation of VSA can be formulated as follows:

$$Q_{\mathcal{F}}, K_{\mathcal{F}}, V_{\mathcal{F}} = X(W_Q, W_K, W_V), \quad (4)$$

$$\text{VSA}(Q_{\mathcal{F}}, K_{\mathcal{F}}, V_{\mathcal{F}}) = \text{Softmax}\left(\frac{Q_{\mathcal{F}}K_{\mathcal{F}}^T}{\sqrt{d}}\right)V_{\mathcal{F}}, \quad (5)$$

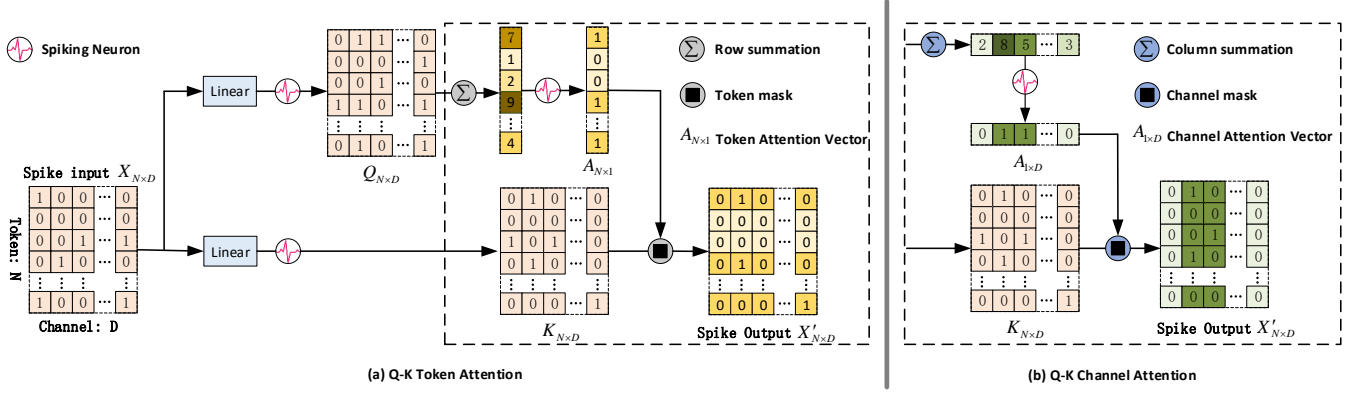


Figure 1: The overview of Q-K attention, which includes two forms: Q-K token attention (QKTA) and Q-K channel attention (QKCA).

where  $\mathcal{F}$  denotes the floating-point form. Both floating-point matrix multiplication and softmax operation which contains exponent calculation and division operation, do not align with the properties of SNNs.

### Spiking Self Attention

Spikformer [Zhou *et al.*, 2023c] demonstrated a novel spike-form self-attention named Spiking Self Attention (SSA), using sparse spike-form  $Q, K, V$  without softmax operation and floating-point matrix multiplication. The calculation process of SSA is formulated as follows:

$$I = \text{SN}_I(\text{BN}_I(X(W_I))), I \in (Q, K, V), \quad (6)$$

$$\text{SSA}'(Q, K, V) = \text{SN}(QK^T V * s), \quad (7)$$

$$\text{SSA}(Q, K, V) = \text{SN}(\text{BN}(\text{Linear}(\text{SSA}'(Q, K, V)))) \quad (8)$$

where  $Q, K, V \in \mathcal{R}^{T \times N \times D}$ , the spike-form  $Q, K, V$  are computed by learnable linear layers.  $s$  is a scaling factor. SN means spiking neuron layer. The calculation of SSA avoids floating-point multiplication, meeting the property of SNNs.

### 3.2 Q-K Attention

An overview of Q-K attention is shown in Figure 1. Both VSA and SSA use three key components and have  $O(N^2d)$  or  $O(Nd^2)$  computational complexity, while our proposed Q-K Attention which has linear complexity and only uses two spike-form components: Query ( $Q$ ) and Key ( $K$ ), which are produced through learnable linear matrices.

$$Q = \text{SN}_Q(\text{BN}(XW_Q)), K = \text{SN}_K(\text{BN}(XW_K)), \quad (9)$$

where  $X$  is the input spiking map. According to the detailed calculation mechanism of  $Q, K$ , Q-K Attention can be divided into Q-K Token Attention (QKTA) and Q-K Channel Attention (QKCA).

#### Q-K Token Attention

We here assume  $T = 1$  and single head attention for mathematical description. After obtaining spike-form  $Q, K \in \mathcal{R}^{T \times N \times D}$ , both  $Q$  and  $K$  can be formed as a spike matrix  $N \times D$  ( $N$  is the token number,  $D$  is the channel number). Q-K Token Attention process can be formulated as follows:

$$A_t = \text{SN}\left(\sum_{i=0}^D Q_{i,j}\right), \quad X' = A_t \otimes K, \quad (10)$$

where  $A_t$  is the  $N \times 1$  token attention vector, which models the binary importance of different tokens.  $A_t$  is a spike-form vector, which is obtained by addition operations (row summation) of  $Q$  spike matrix and a following spiking neuron.  $\otimes$  is the Hadamard product between spike tensors, which is equivalent to the mask operation. We apply the spike-form token attention vector  $A_t$  to the  $K$  spike matrix through the column mask operation (token mask), to obtain the output  $X'$  of Q-K Token Attention.

#### Q-K Channel Attention

The calculation process of Q-K channel attention is similar to the previous Q-K token attention, and can be formulated as follows:

$$A_c = \text{SN}\left(\sum_{j=0}^N Q_{i,j}\right), \quad X' = A_c \otimes K, \quad (11)$$

where  $A_c$  is the  $1 \times D$  channel attention vector, which models the binary importance of different channels.  $A_c$  is a spike-form vector, which is obtained by addition operations (column summation) of  $Q$  spike matrix and a following spiking neuron. Then, the output  $X'$  of Q-K Channel Attention is obtained by the row mask operation (channel mask) between  $A_c$  and  $K$ .

$$X'' = \text{SN}(\text{BN}(\text{Linear}(X'))). \quad (12)$$

As shown in Formula.12, a post-linear layer is also required after obtaining  $X'$  of Q-K Token or Channel Attention. In addition, the channel dimension is  $D/h$  in the multi-head Q-K attention, where  $h$  is the head number. In this work, the spiking neuron uses the LIF model [Fang *et al.*, 2021a]. Same with [Zhou *et al.*, 2023c], time step  $T$  is an independent dimension for the spiking neuron layer. In other layers, it is merged with the batch size. We exploit QKTA in our experiments by default.

#### Discussion on Q-K Attention

**Computational complexity:** As shown in Table 1, the time complexity of Q-K attention varies based on the implementation approach. Specifically, when utilizing spike-form broadcasted element-wise multiplication,  $\otimes$ , the time complexity can reach up to  $O(N * D)$ . When applying mask operation, the time complexity of Q-K attention is only  $O(N)$  or  $O(D)$ .

Methods	Time	Space
VSA	$O(N^2 * D)$	$O(N^2 + ND)$
SSA [Zhou <i>et al.</i> , 2023c]	$O(N^2 * D)$	$O(N^2 + ND)$
SDSA [Yao <i>et al.</i> , 2023]	$O(ND)$	$O(ND)$
QKTA (ours)	$O(D)$	$O(N)$
QKCA (ours)	$O(N)$	$O(D)$

Table 1: Computational complexity comparison.  $N$  is the token number,  $D$  is the channel number.

The space complexity of Q-K attention with the whole process is  $O(N * D)$  at most, which is caused by the self-storage consumption Q and K matrix. In terms of the space complexity of attention operation, Q-K attention only requires an extra  $1 * D$  or  $N * 1$  space to store the attention vector with the space complexity of  $O(N)$  or  $O(D)$ . The linear complexity of Q-K attention makes it possible to successfully explore the large-scale hierarchical architecture SNN model. **Energy efficiency analysis:** All the elements in Q-K attention are in spike-form (either 0 or 1), thus linear multiplication is transformed into sparse addition. Mask operation can be implemented on neuromorphic chips through addressing algorithms [Richter *et al.*, 2022] or AND logic operations [Pei *et al.*, 2019] with negligible power consumption. Compared with SSA, Q-K attention is much more energy-efficient since Q-K attention only adopts two spike-form components for spike [0, 1] operation without the V input and scale operation of SSA and thus has fewer synaptic computing.

### 3.3 QKFormer

As the computational complexity (especially space complexity) of SSA is quadratic to #tokens, previous direct training spiking transformers are all limited to straight-through structures. Combining SSA with hierarchical architecture directly will lead to memory explosion easily when training spiking transformers. To overcome these issues, we proposed a hierarchical spiking transformer based on Q-K attention, named QKFormer, which constructs hierarchical spiking feature maps with linear computational complexity to #tokens or #channels.

#### Overall Hierarchical Architecture

The overview of QKFormer architecture is presented in Figure 2. The input form can be formulated as  $(T_0 \times H \times W \times n)$ . In static RGB image datasets,  $T_0 = 1$  and  $n = 3$ . In temporal neuromorphic datasets, the input  $T_0 = T$ , while  $n = 2$ .

In our implementation, we use a patch size of  $4 \times 4$  and thus the input feature dimension ( $4 \times 4 \times n$ ) of each patch is projected into a spike-form arbitrary dimension (denoted as  $C$ ) in Patch-Embed 1, which together with the following QKFormer blocks are referred to as "Stage 1". The number of tokens in Stage 1 is  $(\frac{H}{4} \times \frac{W}{4})$ .

To produce a hierarchical spiking representation, the number of tokens is reduced in Patch-Embed 2 and Patch-Embed 3 as the network goes deeper. Both Patch-Embed 2 and Patch-Embed 3 reduce the number of tokens by a patch size of  $2 \times 2$  ( $2 \times$  downsampling of resolution), and the number of channels is transformed into  $2C$  and  $4C$ , respectively. We denote

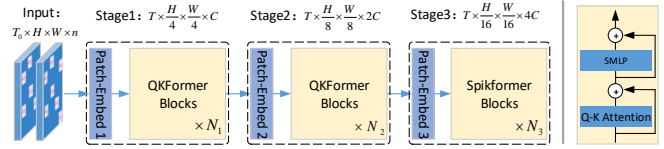


Figure 2: The overview of QKFormer, a hierarchical spiking transformer with Q-K attention. The QKFormer block is shown on the right panel.

the Patch-Embed 2 and the following QKFormer blocks as "Stage 2", which reduces the number of tokens  $(\frac{H}{8} \times \frac{W}{8})$ . While Patch-Embed 3 and the following Spikformer blocks are referred to as "Stage 3" with  $(\frac{H}{16} \times \frac{W}{16})$  tokens. The number of spiking transformer blocks (QKFormer or Spikformer) in each stage are  $N_1$ ,  $N_2$ , and  $N_3$ , respectively. These stages jointly produce a hierarchical spike-form representation.

Similar to the standard transformer encoder block, a QKFormer block contains a Q-K Attention module (QKTA or QKCA) and a Spiking MLP (SMLP) block, which can be formulated as follows:

$$X'_l = \text{QKTA}(X_{l-1}) + X_{l-1}, X'_l \in \mathbf{R}^{T \times N \times D}, \quad (13)$$

$$X_l = \text{SMLP}(X'_l) + X'_l, X_l \in \mathbf{R}^{T \times N \times D}. \quad (14)$$

At last, a fully connected layer (FC) is used for classification.

$$Y = \text{FC}(\text{GAP}(X_L)), \quad (15)$$

where GAP means global average pooling.

#### Patch Embedding with Deformed Shortcut.

The input and output of a patch embedding block have different channel and token numbers. To realize residual learning in patch embedding, we can perform a lightweight linear projection  $W_d$  in the shortcut connections to match the channel and token numbers. Given the input spiking map  $\mathbf{X}$ , the process of patch embedding can be formulated as follows:

$$\mathbf{Y} = \mathcal{F}(\mathbf{X}, \{W_i\}) + \text{SN}(W_d \mathbf{X}). \quad (16)$$

In this work, the deformed linear projection  $W_d$  is set as a lightweight convolutional layer with  $1 \times 1$  kernel and stride  $> 1$ , to meet the channel and token numbers of the patch embedding block. The function  $\mathcal{F}$  involved in this work is set as  $\{\text{Conv2D-BN-MaxPooling-SN-Conv2D-BN-SN}\}$  or  $\{\text{Conv2D-BN-SN-Conv2D-BN-MaxPooling-SN}\}$ , while more layers or more variants are possible.

There are mainly two types of residual shortcuts in deep SNNs. Formula.16 shows the patch embedding in the way of activation-before-addition [Fang *et al.*, 2021a; Zhou *et al.*, 2023c]. The other way of the patch embedding with the pre-activation residual shortcut [Hu *et al.*, 2021; Zhou *et al.*, 2023a; Yao *et al.*, 2023] can be formulated as follows:

$$\mathbf{Y} = \text{SN}(\mathcal{G}(\mathbf{X}, \{W_j\}) + W_d \mathbf{X}), \quad (17)$$

where the function  $\mathcal{G}$  correspondingly could be set as  $\{\text{Conv2D-BN-MaxPooling-SN-Conv2D-BN}\}$  or  $\{\text{Conv2D-BN-SN-Conv2D-BN-MaxPooling}\}$ .

In this work, the patch embedding of stage 2 or stage 3 in QKFormer can be formulated as Formula.16. The patch embedding in stage 1 uses an extra  $\{\text{Conv2D-BN-SN}\}$  for spiking encoding in front of the block (Formula.16) to transform the non-spike input data into spikes.

Dataset	Methods	Architecture	Param (M)	Time Step	Top-1 Acc (%)
ImageNet-1K	SEW ResNet[Fang <i>et al.</i> , 2021a]	SEW-ResNet-34	21.79	4	67.04
		SEW-ResNet-101	44.55	4	68.76
		SEW-ResNet-152	60.19	4	69.26
	MS-ResNet[Hu <i>et al.</i> , 2021]	MS-ResNet-18	11.69	6	63.10
		MS-ResNet-34	21.80	6	69.42
		MS-ResNet-104*	77.28	5	76.02
	Spikformer[Zhou <i>et al.</i> , 2023c]	Spikformer-8-384	16.81	4	70.24
		Spikformer-8-512	29.68	4	73.38
		Spikformer-8-768	66.34	4	74.81
	Spikingformer[Zhou <i>et al.</i> , 2023a]	Spikingformer-8-384	16.81	4	72.45
		Spikingformer-8-512	29.68	4	74.79
		Spikingformer-8-768	66.34	4	75.85
	S-Transformer[Yao <i>et al.</i> , 2023]	S-Transformer-8-384	16.81	4	72.28
		S-Transformer-8-512	29.68	1	71.68
		S-Transformer-8-512	29.68	4	74.57
		S-Transformer-8-768*	66.34	4	77.07
	CML[Zhou <i>et al.</i> , 2023b]	Spikformer-8-384	16.81	4	72.73
		Spikformer-8-512	29.68	4	75.61
		Spikformer-8-768	66.34	4	77.34
	QKFormer	HST-10-384	16.47	4	78.80
HST-10-512		29.08	4	82.04	
HST-10-768		64.96	1	81.69	
HST-10-768		64.96	4	84.22	
HST-10-768*		64.96	4	85.25	
HST-10-768**		64.96	4	<b>85.65</b>	

Table 2: Results on ImageNet-1k classification. \* means 288<sup>2</sup> input resolution when inference, \*\* means 384<sup>2</sup> input and others are 224<sup>2</sup> by default. The top-5 accuracy of QKFormer (HST-10-768\*\*) is 97.74%.

## 4 Experiments

In this section, we first evaluate the classification performance of our proposed QKFormer on the large-scale image dataset, ImageNet-1K [Deng *et al.*, 2009]. Then, we assess the performance of QKFormer on small-scale static datasets, CIFAR [Krizhevsky, 2009] (including CIFAR10 and CIFAR100). Furthermore, we examine QKFormer on popular temporal neuromorphic datasets, including CIFAR10-DVS [Li *et al.*, 2017] and DVS128 Gesture [Amir *et al.*, 2017]. Finally, we conduct a series of ablation studies to further understand the model.

### 4.1 Results on ImageNet-1k Classification

In this experiment, we use AdamW as the optimizer, which is adopted with a base learning rate of  $6 \times 10^{-4}$ . The actual learning rate was calculated as  $\text{BatchSize}/256$  multiplied by the base learning rate. The batch size is set to 512, which is realized by accumulated gradient iterations [He *et al.*, 2022] and distributed across 8 Nvidia V100 GPUs. We trained QKFormer for 200 epochs. In addition, following DeiT [Touvron *et al.*, 2021], data augmentation techniques including RandAugment [Cubuk *et al.*, 2020], random erasing [Zhong *et al.*, 2020], and stochastic depth [Huang *et al.*, 2016] are employed in this study. The number of blocks in the three stages is set as  $\{1, 2, 7\}$  respectively. The architecture

of QKFormer is named Hierarchical Spiking Transformer (HST). The ImageNet-1k classification results of QKFormer are shown in Table 2. Note that SEW ResNet, Spikformer, CML and our QKFormer in this experiment are all based on activation-before-addition shortcuts, while MS ResNet, Spikingformer, and S-Transformer are all based on the pre-activation shortcuts.

The experimental results demonstrate the superior performance of our proposed QKFormer, surpassing previous works’ performance by a large margin (Table 2). QKFormer (**64.96 M**) achieves **85.65%** top-1 accuracy and **97.74%** top-5 accuracy on ImageNet. To begin with, we compare our model with the baseline spiking transformer (i.e., Spikformer [Zhou *et al.*, 2023c]). Our QKFormer models have slightly fewer parameters but much higher performance. For example, our QKFormer (64.96 M, 85.65%) significantly outperforms Spikformer (66.34 M, 74.81%) by **10.84%**. In addition, compared with SDSA, our Q-K attention has lower computational complexity (shown in Table 1) and our QKFormer has much higher performance than S-Transformer (built by SDSA) [Yao *et al.*, 2023]. In detail, QKFormer outperforms S-Transformer by 7.55%, 7.47%, and 8.58% respectively on three models with comparable #parameters. Finally, Our QKFormer outperforms the SOTA model CML [Zhou *et al.*, 2023b] by 6.07%, 6.43%, and 8.31% respectively on three

Dataset	Methods	Architecture	Param (M)	Time Step	Top-1 Acc (%)
CIFAR10	Spikformer[Zhou <i>et al.</i> , 2023c]	Spikformer-4-384	9.32	4	95.51
	Spikingformer[Zhou <i>et al.</i> , 2023a]	Spikingformer-4-384	9.32	4	95.81
	CML[Zhou <i>et al.</i> , 2023b]	Spikformer-4-384	9.32	4	96.04
	S-Transformer[Yao <i>et al.</i> , 2023]	S-Transformer-2-512	10.28	4	95.60
	<b>QKFormer</b>	HST-4-384	6.74	4	<b>96.18</b>
CIFAR100	Spikformer[Zhou <i>et al.</i> , 2023c]	Spikformer-4-384	9.32	4	78.21
	Spikingformer[Zhou <i>et al.</i> , 2023a]	Spikingformer-4-384	9.32	4	78.21
	CML[Zhou <i>et al.</i> , 2023b]	Spikformer-4-384	9.32	4	80.02
	S-Transformer[Yao <i>et al.</i> , 2023]	S-Transformer-2-512	10.28	4	78.4
	<b>QKFormer</b>	HST-4-384	6.74	4	<b>81.15</b>
DVS128	Spikformer[Zhou <i>et al.</i> , 2023c]	Spikformer-2-256	2.57	10 / 16	96.9 / 98.3
	Spikingformer[Zhou <i>et al.</i> , 2023a]	Spikingformer-2-256	2.57	10 / 16	96.2 / 98.3
	CML[Zhou <i>et al.</i> , 2023b]	Spikformer-2-256	2.57	10 / 16	97.6 / 98.6
	S-Transformer[Yao <i>et al.</i> , 2023]	S-Transformer-2-256	2.57	- / 16	- / <b>99.3</b>
	STSA[Wang <i>et al.</i> , 2023]	STSFormer-2-256	1.99	10 / 16	97.3 / 98.7
	<b>QKFormer</b>	HST-2-256	1.50	10 / 16	98.3 / 98.6
CIFAR10-DVS	Spikformer[Zhou <i>et al.</i> , 2023c]	Spikformer-2-256	2.57	10 / 16	78.9 / 80.9
	Spikingformer[Zhou <i>et al.</i> , 2023a]	Spikingformer-2-256	2.57	10 / 16	79.9 / 81.3
	CML[Zhou <i>et al.</i> , 2023b]	Spikformer-2-256	2.57	10 / 16	79.2 / 80.9
	S-Transformer[Yao <i>et al.</i> , 2023]	S-Transformer-2-256	2.57	- / 16	- / 80.0
	STSA[Wang <i>et al.</i> , 2023]	STSFormer-2-256	1.99	10 / 16	78.96 / 79.93
	<b>QKFormer</b>	HST-2-256	1.50	10 / 16	83.8 / <b>84.0</b>

Table 3: Comparison on CIFAR10, CIFAR100, DVS128, CIFAR10-DVS.

models with comparable #parameters. To our best knowledge, this is the first time that a direct training SNN model has achieved an accuracy of over **85%** on ImageNet-1k.

## 4.2 Results on Small Dataset Classification

We evaluate our QKFormer on small-scale datasets, including CIFAR10, CIFAR100 [Krizhevsky, 2009] and temporal neuromorphic datasets (CIFAR10-DVS and DVS128 Gesture [Amir *et al.*, 2017]). The overview results on the four small-scale datasets are presented in Table 3.

### CIFAR Classification

In this experiment, the QKFormer is trained for 400 epochs with a batch size of 64 following previous works: Spikformer [Zhou *et al.*, 2023c], Spikingformer [Zhou *et al.*, 2023a]. Following Spikformer, we use 4 blocks in QKFormer in total, which are distributed  $\{1, 1, 2\}$  in three stages. Due to the hierarchical architecture design, our QKFormer model has only 6.74 M parameters in this case.

The results on CIFAR datasets are shown in Table 3. For CIFAR10, our model achieved **96.18%** accuracy with **6.74 M** parameters. Our proposed QKFormer outperforms Spikformer by 0.67% and reduces 2.58 M parameters meanwhile.

For CIFAR100, our model achieved **81.15%** with 6.74 M parameters. Our proposed QKFormer outperforms Spikformer by **2.94%** and reduces 2.58 M parameters meanwhile.

### Temporal Neuromorphic Classification

We compare our method with SOTA methods on both CIFAR10-DVS and DVS-Gesture datasets. In this experiment, We utilize a mini QKFormer model with 1.50 M parameter, which has  $\{0, 1, 1\}$  blocks in three stages. The max patch embedding dimension is set to 256. The training process involves 200 epochs for DVS128 Gesture and 106 epochs for CIFAR10-DVS. The number of time steps of the spiking neuron is 10 or 16.

The experimental results of temporal neuromorphic classification are presented in Table 3. For DVS128-Gesture dataset, our model with 1.50 M parameters achieves 98.6% accuracy using 16 time steps and 98.3% accuracy using 10 time steps. For CIFAR10-DVS dataset, our model achieves **84.0%** accuracy with only **1.50 M** parameters using 16 time steps. Our proposed QKFormer significantly outperforms Spikformer by **3.1%** while reducing 1.07 M parameters. In addition, our model with 10 time steps achieves 83.8% accuracy, which outperforms Spikformer by **4.9%** and outper-



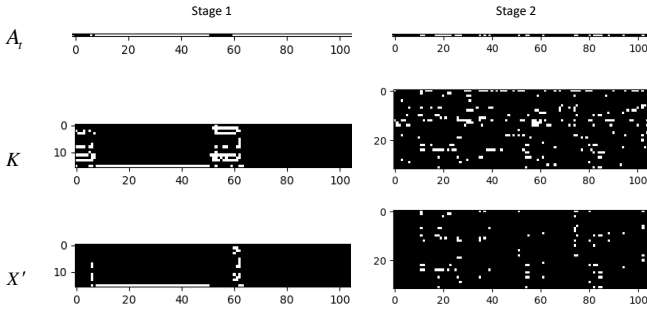


Figure 3: The visualization of Q-K token attention. The white dot means value 1, while the black one means value 0.

forms the SOTA model (Spikingformer) by 3.9%.

### 4.3 Analyses on Q-K Attention

#### Visualization

In this part, we visualize the Q-K token attention (Stage 1 and Stage 2 of the QKFormer model) on ImageNet. As shown in Figure 3,  $A_t$  is the  $N * 1$  token attention vector, and  $X'$  is the output of the attention process, which is obtained by the mask operation between matrix  $K$  and attention vector  $A_t$ . Specifically, the longitudinal axis denotes the channel index of one head, while the horizontal axis denotes the token index. The #tokens in stage 1 and stage 2 are  $56^2$  and  $28^2$ , respectively. To facilitate visualization, we choose a continuous segment with a length of 100 extracted from the whole token vector. The visualization shows Q-K attention can lead to high sparsity of spikes.

#### Memory Consumption

In this experiment, we compare the memory consumption between QKTA (Formula.10) and SSA (Formula.7) under different token numbers. We calculate the memory consumption of a QKTA and an SSA on a GPU by forwarding the input tensor  $(T, B, C, N)$ . To facilitate the statistics of the impact of #tokens  $N$  on memory consumption, the #channels  $C$  is set to 256, and the time step  $T$  and batch size  $B$  are set to 1. The experiment result is shown in Figure 4. With the increment of #Tokens, SSA consumes much more GPU memory than

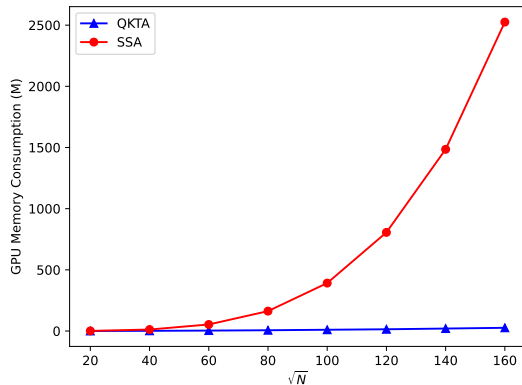


Figure 4: Comparison of memory costs between QKTA and SSA under different token numbers.  $N$  is the token number.

QKTA, of which the complexity is linear to #Tokens. For example, SSA consumes about  $10 \times$  GPU memory than QKTA when  $\sqrt{N} = 50$ .

### 4.4 Verification on PEDS Module

In this experiment, we conduct the ablation study for our Patch Embedding module with Deformed Shortcut (PEDS) on CIFAR100 and CIFAR10-DVS datasets. We replaced the

Dataset	CIFAR100	CIFAR10-DVS
Spikformer	78.21%	80.9%
Spikformer + PEDS	80.26%	82.2%

Table 4: Ablation study results of PEDS on CIFAR100 and CIFAR10-DVS dataset.

Spiking Patch Splitting (SPS) module in Spikformer with our PEDS module, while other conditions remain unchanged. The experimental results, shown in Table 4, indicate that our PEDS module brings a great gain in CIFAR100 (+2.05%) and CIFAR10-DVS (+1.3%) compared to the baseline.

### 4.5 Effects of Time Step

The performance of QKFormer with different simulation time steps of spiking neurons is shown in Table 5. Actually, within a certain range, the larger the time step ( $T$ ), the better the performance. In addition, our model with  $T=1$  is only 2.64% lower than the model with  $T=4$  on CIFAR100, demonstrating that QKFormer is robust under low latency conditions.

Time step	T=1	T=2	T=4	T=6
QKFormer	78.51%	80.08%	81.15%	81.30%

Table 5: The results of QKFormer with different time steps on CIFAR100 classification.

## 5 Conclusion

In this work, we design a novel spike-form Q-K attention considering the properties of SNNs, which can easily model the importance of token or channel dimensions through binary vectors. Q-K attention has linear complexity to #tokens (or #channels) and only adopts two spike-form components: Query ( $Q$ ) and Key ( $K$ ). We design a versatile and powerful Patch Embedding module with a Deformed Shortcut (PEDS), which can improve the performance of spiking transformers greatly. In addition, we develop a hierarchical spiking transformer based on the proposed Q-K attention and PEDS in a direct training way, named QKFormer, which marks the effective exploration of hierarchical spiking representation in Transformer-based SNNs. Extensive experiments show that the proposed model achieves SOTA performance on both static and neuromorphic datasets. Note that QKFormer achieved top-1 accuracy beyond 85% on ImageNet-1k with 4 time steps using the direct training way for the first time. With its powerful performance, we aim for our investigations to instill optimism in the application of SNNs.

## References

- [Amir *et al.*, 2017] Arnon Amir, Brian Taba, David Berg, Timothy Melano, Jeffrey McKinstry, Carmelo Di Nolfo, Tapan Nayak, Alexander Andreopoulos, Guillaume Garreau, Marcela Mendoza, Jeff Kusnitz, Michael Debole, Steve Esser, Tobi Delbruck, Myron Flickner, and Dharmendra Modha. A low power, fully event-based gesture recognition system. In *Proceedings of the IEEE/CVF Conference on Computer Vision and Pattern Recognition (CVPR)*, pages 7243–7252, 2017.
- [Bu *et al.*, 2021] Tong Bu, Wei Fang, Jianhao Ding, PengLin Dai, Zhaofei Yu, and Tiejun Huang. Optimal ann-snn conversion for high-accuracy and ultra-low-latency spiking neural networks. In *International Conference on Learning Representations (ICLR)*, 2021.
- [Burkitt, 2006] Anthony N Burkitt. A review of the integrate-and-fire neuron model: I. homogeneous synaptic input. *Biological cybernetics*, 95:1–19, 2006.
- [Cubuk *et al.*, 2020] Ekin D Cubuk, Barret Zoph, Jonathon Shlens, and Quoc V Le. Randaugment: Practical automated data augmentation with a reduced search space. In *Proceedings of the IEEE/CVF conference on computer vision and pattern recognition workshops*, pages 702–703, 2020.
- [Deng *et al.*, 2009] Jia Deng, Wei Dong, Richard Socher, Li-Jia Li, Kai Li, and Li Fei-Fei. Imagenet: A large-scale hierarchical image database. In *Proceedings of the IEEE/CVF Conference on Computer Vision and Pattern Recognition (CVPR)*, pages 248–255, 2009.
- [Dosovitskiy *et al.*, 2020] Alexey Dosovitskiy, Lucas Beyer, Alexander Kolesnikov, Dirk Weissenborn, Xiaohua Zhai, Thomas Unterthiner, Mostafa Dehghani, Matthias Minderer, Georg Heigold, Sylvain Gelly, et al. An image is worth 16x16 words: Transformers for image recognition at scale. In *International Conference on Learning Representations (ICLR)*, 2020.
- [Fang *et al.*, 2021a] Wei Fang, Zhaofei Yu, Yanqi Chen, Tiejun Huang, Timothée Masquelier, and Yonghong Tian. Deep Residual Learning in Spiking Neural Networks. In *Proceedings of the International Conference on Neural Information Processing Systems (NeurIPS)*, volume 34, pages 21056–21069, 2021.
- [Fang *et al.*, 2021b] Wei Fang, Zhaofei Yu, Yanqi Chen, Timothee Masquelier, Tiejun Huang, and Yonghong Tian. Incorporating learnable membrane time constant to enhance learning of spiking neural networks. In *Proceedings of the IEEE/CVF International Conference on Computer Vision (ICCV)*, pages 2661–2671, October 2021.
- [Hao *et al.*, 2023] Zecheng Hao, Jianhao Ding, Tong Bu, Tiejun Huang, and Zhaofei Yu. Bridging the gap between anns and snns by calibrating offset spikes. *ArXiv*, abs/2302.10685, 2023.
- [He *et al.*, 2022] Kaiming He, Xinlei Chen, Saining Xie, Yanghao Li, Piotr Dollár, and Ross Girshick. Masked autoencoders are scalable vision learners. In *Proceedings of the IEEE/CVF conference on computer vision and pattern recognition*, pages 16000–16009, 2022.
- [Hu *et al.*, 2021] Yifan Hu, Yujie Wu, Lei Deng, and Guoqi Li. Advancing residual learning towards powerful deep spiking neural networks. *arXiv preprint arXiv:2112.08954*, 2021.
- [Huang *et al.*, 2016] Gao Huang, Yu Sun, Zhuang Liu, Daniel Sedra, and Kilian Q Weinberger. Deep networks with stochastic depth. In *Computer Vision—ECCV 2016: 14th European Conference, Amsterdam, The Netherlands, October 11–14, 2016, Proceedings, Part IV 14*, pages 646–661. Springer, 2016.
- [Krizhevsky, 2009] Alex Krizhevsky. Learning multiple layers of features from tiny images. 2009.
- [Li *et al.*, 2017] Hongmin Li, Hanchao Liu, Xiangyang Ji, Guoqi Li, and Luping Shi. Cifar10-dvs: an event-stream dataset for object classification. *Frontiers in neuroscience*, 11:309, 2017.
- [Li *et al.*, 2021] Yuhang Li, Shi-Wee Deng, Xin Dong, Ruihao Gong, and Shi Gu. A free lunch from ann: Towards efficient, accurate spiking neural networks calibration. *ArXiv*, abs/2106.06984, 2021.
- [Liu *et al.*, 2021] Ze Liu, Yutong Lin, Yue Cao, Han Hu, Yixuan Wei, Zheng Zhang, Stephen Lin, and Baining Guo. Swin transformer: Hierarchical vision transformer using shifted windows. In *Proceedings of the IEEE/CVF International Conference on Computer Vision (ICCV)*, pages 10012–10022, 2021.
- [Maass, 1997] Wolfgang Maass. Networks of spiking neurons: the third generation of neural network models. *Neural networks*, 10(9):1659–1671, 1997.
- [Neftci *et al.*, 2019] Emre O Neftci, Hesham Mostafa, and Friedemann Zenke. Surrogate gradient learning in spiking neural networks: Bringing the power of gradient-based optimization to spiking neural networks. *IEEE Signal Processing Magazine*, 36(6):51–63, 2019.
- [Pei *et al.*, 2019] Jing Pei, Lei Deng, Sen Song, Mingguo Zhao, Youhui Zhang, Shuang Wu, Guanrui Wang, Zhe Zou, Zhenzhi Wu, Wei He, et al. Towards artificial general intelligence with hybrid tianjic chip architecture. *Nature*, 572(7767):106–111, 2019.
- [Richter *et al.*, 2022] Ole Juri Richter, QIAO Ning, Qian Liu, and Sadique Ul Ameen Sheik. Event-driven spiking convolutional neural network, June 16 2022. US Patent App. 17/601,939.
- [Roy *et al.*, 2019] Kaushik Roy, Akhilesh Jaiswal, and Priyadarshini Panda. Towards spike-based machine intelligence with neuromorphic computing. *Nature*, 575(7784):607–617, 2019.
- [Touvron *et al.*, 2021] Hugo Touvron, Matthieu Cord, Matthijs Douze, Francisco Massa, Alexandre Sablayrolles, and Hervé Jégou. Training data-efficient image transformers & distillation through attention. In *International conference on machine learning*, pages 10347–10357. PMLR, 2021.



- [Vaswani *et al.*, 2017] Ashish Vaswani, Noam Shazeer, Niki Parmar, Jakob Uszkoreit, Llion Jones, Aidan N Gomez, Łukasz Kaiser, and Illia Polosukhin. Attention is all you need. In *Proceedings of the International Conference on Neural Information Processing Systems (NeurIPS)*, volume 30, 2017.
- [Wang *et al.*, 2021] Rong Wang, Mianxin Liu, Xinhong Cheng, Ying Wu, Andrea Hildebrandt, and Changsong Zhou. Segregation, integration, and balance of large-scale resting brain networks configure different cognitive abilities. *Proceedings of the National Academy of Sciences*, 118(23):e2022288118, 2021.
- [Wang *et al.*, 2023] Yuchen Wang, Kexin Shi, Chengzhuo Lu, Yuguo Liu, Malu Zhang, and Hong Qu. Spatial-temporal self-attention for asynchronous spiking neural networks. In Edith Elkind, editor, *Proceedings of the Thirty-Second International Joint Conference on Artificial Intelligence, IJCAI-23*, pages 3085–3093. International Joint Conferences on Artificial Intelligence Organization, 8 2023. Main Track.
- [Wu *et al.*, 2018] Yujie Wu, Lei Deng, Guoqi Li, Jun Zhu, and Luping Shi. Spatio-temporal backpropagation for training high-performance spiking neural networks. *Frontiers in neuroscience*, 12:331, 2018.
- [Xiao *et al.*, 2021] Mingqing Xiao, Qingyan Meng, Zongpeng Zhang, Yisen Wang, and Zhouchen Lin. Training feedback spiking neural networks by implicit differentiation on the equilibrium state. In *Proceedings of the International Conference on Neural Information Processing Systems (NeurIPS)*, volume 34, pages 14516–14528, 2021.
- [Yao *et al.*, 2023] Man Yao, Jiakui Hu, Zhaokun Zhou, Li Yuan, Yonghong Tian, Bo Xu, and Guoqi Li. Spike-driven transformer, 2023.
- [Zheng *et al.*, 2021] Hanle Zheng, Yujie Wu, Lei Deng, Yifan Hu, and Guoqi Li. Going Deeper With Directly-Trained Larger Spiking Neural Networks. In *Proceedings of the AAAI Conference on Artificial Intelligence (AAAI)*, pages 11062–11070, 2021.
- [Zhong *et al.*, 2020] Zhun Zhong, Liang Zheng, Guoliang Kang, Shaozi Li, and Yi Yang. Random erasing data augmentation. In *Proceedings of the AAAI conference on artificial intelligence*, volume 34, pages 13001–13008, 2020.
- [Zhou *et al.*, 2023a] Chenlin Zhou, Liutao Yu, Zhaokun Zhou, Han Zhang, Zhengyu Ma, Huihui Zhou, and Yonghong Tian. Spikingformer: Spike-driven residual learning for transformer-based spiking neural network, 2023.
- [Zhou *et al.*, 2023b] Chenlin Zhou, Han Zhang, Zhaokun Zhou, Liutao Yu, Zhengyu Ma, Huihui Zhou, Xiaopeng Fan, and Yonghong Tian. Enhancing the performance of transformer-based spiking neural networks by improved downsampling with precise gradient backpropagation, 2023.
- [Zhou *et al.*, 2023c] Zhaokun Zhou, Yuesheng Zhu, Chao He, Yaowei Wang, Shuicheng YAN, Yonghong Tian, and

Li Yuan. Spikformer: When spiking neural network meets transformer. In *The Eleventh International Conference on Learning Representations*, 2023.

## A Appendix

### A.1 Experimental Details

#### Datasets

We evaluate QKFormer on static image classification and neuromorphic classification. The former includes ImageNet-1K [Deng *et al.*, 2009], CIFAR10/100 [Krizhevsky, 2009]. The latter contains CIFAR10-DVS [Li *et al.*, 2017] and DVS128 Gesture [Amir *et al.*, 2017].

ImageNet-1K is the most typical static image dataset for classification. It contains 1.28 million images for training and 50k images for validation, with a total of 1,000 categories. CIFAR10/CIFAR100 provides 50, 000 train and 10, 000 test images with  $32 \times 32$  resolution. The difference is that CIFAR10 contains 10 categories for classification. While CIFAR100 contains 100 categories, owning better distinguishing ability for the classification algorithm.

CIFAR10-DVS is an event-based neuromorphic dataset converted from the static image dataset by capturing shifting image samples through the Dynamic Vision Sensor (DVS) camera, which provides 9,000 training samples and 1,000 test samples. DVS128 Gesture is an event-based gesture recognition dataset that contains 1342 samples of 11 hand gesture categories from 29 individuals under 3 illumination conditions, each gesture has an average duration of 6 seconds.

#### Training Details.

In our experiments, we use 8 NVIDIA Tesla V100 SXM2 32GB GPUs when training models on ImageNet, while 1 GPU is used to train other datasets (CIFAR10, CIFAR100, DVS128 Gesture, CIFAR10-DVS). In direct training SNN models with surrogate function,

$$\sigma(x) = \frac{1}{1 + \exp(-\alpha x)}, \quad (18)$$

we select the Sigmoid function  $\sigma(x)$  as the surrogate function with  $\alpha = 4$  during the backpropagation of direct training in all experiments.

### A.2 Q-K Channel Attention

In this experiment, we show three combination strategies of QKCA, QKTA, and SSA. The baseline is our QKFormer, which has 4 blocks, distributed in three stages  $\{1, 1, 2\}$ . The former two blocks use QKTA, and the latter two blocks use SSA. Similarly, we conducted the combination of "QKCA + SSA" and "QKTA + QKCA" on CIFAR 100, the experimental results are shown in Table 6.

Model	QKFormer	QKCA+SSA	QKTA+QKCA
Parameter	6.70 M	6.70 M	6.44 M
CIFAR100	81.15%	81.07%	81.04%

Table 6: Ablation study results of Q-K attention on CIFAR 100.

The experimental results show that the three combination strategies have comparable performance on CIFAR 100. Compared with the baseline QKFormer (QKTA + SSA, 6.70 M, 81.15%), both the number of parameters and the classification accuracy of "QKTA + QKCA" (6.44 M, 81.04%) are reduced. Actually, from our experimental practices, we could choose the one with a larger length of the attention vector for specified network layers when applying QKTA or QKCA to build networks.

### A.3 Spike Firing Rates in QKFormer Blocks

In this experiment, we calculate the spike firing rates of QKFormer blocks of the trained QKFormer (64.9M) on the ImageNet-1K test set with the  $224 \times 224$  input resolution. The average spike firing rates of the QKFormer blocks in Stage1 and Stage2 are shown in Table 7.

QKFormer Block		Stage1	Stage2
QKTA	$Q$	0.0432	0.0231
	$K$	0.1784	0.0847
	$A_t$	0.3477	0.2655
	$X'$	0.0832	0.0350
	$X''$	0.1478	0.0577
SMLP	Layer1	0.0518	0.0246
	Layer2	0.2733	0.1869

Table 7: Spike firing rates in QKFormer blocks. Note that the spike-form  $X'$  is obtained by column mask operation (token mask) between  $A_t$  and  $K$ .

$\sqrt{N}$	QKTA (M)	SSA (M)	SSA / QKTA
10	0.10	0.14	1.37
20	0.40	1.00	2.53
30	0.89	3.97	4.46
40	1.58	12.19	7.71
50	2.47	26.44	10.70
60	3.56	53.52	15.04
70	4.84	97.64	20.17
80	6.32	162.50	25.70
90	8.18	258.19	31.55
100	10.35	391.77	37.85
110	12.14	570.69	47.01
120	14.23	806.06	56.66
130	16.70	1107.50	66.33
140	20.22	1485.14	73.43
150	22.26	1954.03	87.79
160	26.29	2525.00	96.03
170	28.55	3214.30	112.57
180	32.37	4036.88	124.71
190	36.41	5007.25	137.51
200	40.46	6143.06	151.84

Table 8: Detailed values of memory consumption of Figure 4 in the main body of this paper.

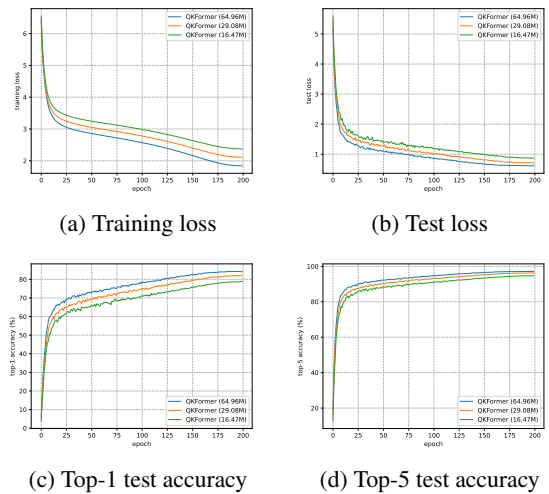


Figure 5: Training loss, test loss, top-1 and top-5 test accuracy of QKFormer on ImageNet-1K. The input resolution of training and testing are  $224 \times 224$ .

### A.4 Supplementary for Memory Consumption in Experiment 4.3

Table 8 shows the detailed values of Figure 4 in the main body of this paper (Experiment 4.3).

### A.5 QKFormer with Other Spiking Neurons

Table 9 shows the results of QKFormer with other spiking neuron models: IF [Burkitt, 2006] and Parametric LIF (PLIF) [Fang *et al.*, 2021b]. The time steps of models on CIFAR100 and DVS128 are 4 and 16, respectively.

Dataset	CIFAR100	DVS128
QKFormer (IF)	80.95%	96.9%
QKFormer (PLIF)	81.12%	98.3%

Table 9: The results of QKFormer with other spiking neuron models on CIFAR100 and DVS128.

### A.6 Performance Discussion on ImageNet

We show the training loss, test loss, top-1, and top-5 test accuracy of QKFormer (64.96M, 29.08M, 16.47M) on ImageNet-1K in Figure 5. Our QKFormer is a directly trained event-driven SNN on the ImageNet-1K. Under the same experiment conditions without pre-training or extra training data, our QKFormer has surpassed most well-known Transformer-based ANNs with high-power MAC operation: QKFormer (64.96M, 85.65%, SNN) > Swin Transformer(88M, 84.5%, ANN) [Liu *et al.*, 2021] > DeiT-B (86M, 83.1%, ANN) [Touvron *et al.*, 2021] > ViT (85.9M, 77.9%, ANN) [Dosovitskiy *et al.*, 2020].